ASBMB JOURNAL OF LIPID RESEARCH

The effect of phospholipid composition of reconstituted HDL on its cholesterol efflux and anti-inflammatory properties[S]

Anna Schwendeman,[1,*] Denis O. Sviridov,[†] Wenmin Yuan,[*] Yanhong Guo,[§] Emily E. Morin,[*] Yue Yuan,[*,] John Stonik,[†] Lita Freeman,[†] Alice Ossoli,[†] Seth Thacker,[†] Salena Killion,[††] Milton Pryor,[†] Y. Eugene Chen,[§] Scott Turner,[††] and Alan T. Remaley[†]**

Department of Medicinal Chemistry and the Biointerfaces Institute,[*] and Department of Cardiac Surgery,[§] University of Michigan, Ann Arbor, MI 48109; National Heart, Lung, and Blood Institute,[†] National Institutes of Health, Bethesda, MD 20892; School of Pharmacy,[**] Shenyang Pharmaceutical University, Shenyang 110016, People's Republic of China; and KineMed, Inc.,[††] Emeryville, CA 94608

Abstract **The goal of this study was to understand how the reconstituted HDL (rHDL) phospholipid (PL) composition affects its cholesterol efflux and anti-inflammatory properties. An ApoA-I mimetic peptide, 5A, was combined with either SM or POPC. Both lipid formulations exhibited similar in vitro cholesterol efflux by ABCA1, but 5A-SM exhibited higher ABCG1- and SR-BI-mediated efflux relative to 5A-POPC ($P < 0.05$). Injection of both rHDLs in rats resulted in mobilization of plasma cholesterol, although the relative potency was 3-fold higher for the same doses of 5A-SM than for 5A-POPC. Formation of preβ HDL was observed following incubation of rHDLs with both human and rat plasma in vitro, with 5A-SM inducing a higher extent of preβ formation relative to 5A-POPC. Both rHDLs exhibited anti-inflammatory properties, but 5A-SM showed higher inhibition of TNF-α, IL-6, and IL-1β release than did 5A-POPC ($P < 0.05$). Both 5A-SM and 5A-POPC showed reduction in total plaque area in ApoE$^{-/-}$ mice, but only 5A-SM showed a statistically significant reduction over placebo control and baseline ($P < 0.01$). The type of PL used to reconstitute peptide has significant influence on rHDL's anti-inflammatory and anti-atherosclerosis properties.**—Schwendeman, A., D. O. Sviridov, W. Yuan, Y. Guo, E. E. Morin, Y. Yuan, J. Stonik, L. Freeman, A. Ossoli, S. Thacker, S. Killion, M. Pryor, Y. E. Chen, S. Turner, and A. T. Remaley. **The effect of phospholipid composition of reconstituted HDL on its cholesterol efflux and anti-inflammatory properties.** ***J. Lipid Res.*** **2015.** 56: **1727–1737.**

Supplementary key words high density lipoprotein • apolipoprotein A-I • sphingomyelin • peptides • inflammation • atherosclerosis

Infusions of cholesterol-free reconstituted HDL (rHDL) particles have been shown to rapidly reverse atherosclerosis in a wide variety of animal models and in clinical trials of acute coronary syndrome patients (1–5). While a significant emphasis has been placed on investigating the HDL protein component, i.e., ApoA-I, ApoA-I mutants, and mimetic peptides, the importance of HDL phospholipid (PL) composition has not been systematically investigated. Lipid represents 50–80% of the total HDL mass and is known to affect particle stability in vivo, cholesterol efflux from macrophages, the ability to interact with LCAT, and cholesterol elimination (6–11). Lipid composition also largely defines the size, net charge, and rigidity of the rHDL particles; all are important factors in the pharmacokinetic and pharmacodynamic properties of rHDL. The investigation of the effects of lipid composition on the resulting rHDL properties in vitro and in vivo is the focus of this article. By better defining the lipid effect of rHDL, we hope to be able to favorably alter the potency and safety of rHDL, and ultimately advance clinical translation of these potentially life-changing nanomedicines.

The PL composition of endogenous HDL contains phosphatidylcholines (PCs), SM, and small amounts of lysophosphatidylcholine (LPC), phosphatidylethanolamine,

This research was funded in part by American Heart Association Grants 13SDG17230049, R01 GM113832, R01 HL068878, and R01 HL117491. E.E.M. was supported by a Cellular Biotechnology Training Program T32 GM008353. Y.Y. was supported by grant 81202481 of the National Natural Science for Youth Foundation of China and grant GGJJ2014102 of the Scientific Research Foundation for the Returned Overseas Chinese Scholars by Shenyang Pharmaceutical University.

Manuscript received 29 April 2015 and in revised form 25 June 2015.

Published, JLR Papers in Press, June 27, 2015
DOI 10.1194/jlr.M060285

Abbreviations: BHK, baby hamster kidney; CD, circular dichroism; CE, cholesterol ester; DLnPC, 1,2-dilinolenoyl phosphatidylcholine; DLPC, 1,2-dilinoleoyl phosphatidylcholine; DLS, dynamic light scattering; DMPC, 1,2-dimyristoyl-rac-glycero-3-phosphocholine; DOPC, 1,2-dioleoyl phosphatidylcholine; DPPC, 1,2-dipalmitoyl-*sn*-glycero-3-phosphocholine; DSPC, 1,2-distearoyl-phosphatidylcholine; FC, free cholesterol; LPC, lysophosphatidylcholine; LPS, lipopolysaccharide; PC, phosphatidylcholine; PHA, phytohemaglutinin-M; PL, phospholipid; rHDL, reconstituted HDL; soyPC, soybean phosphatidylcholine; TBE, Tris borate EDTA; TC, total cholesterol; TEM, transmission electron microscopy.

[1] To whom correspondence should be addressed.
e-mail: annaschw@umich.edu

[S] The online version of this article (available at http://www.jlr.org) contains a supplement.

phosphatidylinositol, and other lipids (12–14). The differences in lipid composition of various subclasses of HDL and how they relate to disease have been gaining attention in recent years (12–14). However, a single source of lipid is used for preparation of rHDL for most academic research and clinical development (2–5, 15–18). The first lipid used to prepare rHDLs for human testing was soybean PC (soyPC), because this lipid was shown to be safe for parenteral nutrition products and is readily commercially available in infusion grade (18). Thus recombinant proApoA-I (a product of UCB Pharma, Anderlecht, Belgium) and blood purified ApoA-I (CSL-111, a product of CSL Behring, Australia) were reconstituted with soyPC (15, 16). As a greater variety of infusion grade chemically defined lipids became commercially available, the PL composition used in the preparation of rHDL diversified. A POPC was first used in ETC-216 (rApoA-I-Milano), and then a mixture of 1,2-dipalmitoyl-*sn*-glycero-3-phosphocholine (DPPC) and SM was used for ETC-642, a peptide-based rHDL (17, 19). Most recently, SM was used in CER-001, another newly developed rApoA-I-based rHDL (20). Both SM and saturated fatty acid-containing lipids like DPPC have superior cholesterol binding capacity relative to unsaturated POPC and soyPC (21, 22). In fact, SM has the strongest cholesterol binding affinity governed by Van der Waals' interaction due to the mismatched fatty acid lengths (21). SM is also known to form lipid-raft sections in cellular membrane that contain up to 50% cholesterol (23). The rHDLs made from saturated lipids exhibited greater cholesterol efflux from macrophages in vitro (8, 9) and cholesterol mobilization in vivo (24). However, unsaturation enhances rHDL interaction with LCAT (11), whereas SM was reported to inhibit cholesterol esterification in vitro (6).

In this study, we hypothesized that the higher cholesterol binding affinity of SM relative to POPC would translate into greater cholesterol efflux both in vitro and in vivo. The ApoA-I mimetic, 5A, a 37-amino acid-long bihelical peptide (25), was used to form SM- and POPC-based HDL particles. The 5A-based HDL has several similar features to HDL prepared from the full-length ApoA-I, namely, an equivalent ability to promote cholesterol efflux in vitro and in vivo (25, 26), and similar abilities in reducing the development of atherosclerosis (26) and suppressing inflammation (27). In this study, differences in cholesterol efflux and inflammatory cytokine release inhibition were examined for 5A-POPC and 5A-SM. In addition, the ability of the two different lipid preparations of 5A were tested in vivo on their ability to mobilize and esterify cholesterol and on their effect in atherosclerosis development.

MATERIALS AND METHODS

Materials

5A (DWLKAFYDKVAEKLKEAFPDWAKAAYDKAAEKAKEAA) was synthesized by GenScript (Piscataway, NJ), using solid-phase 9-fluorenylmethyl carbamate protection chemistry and was purified with reverse phase chromatography. Peptide purity was >95%, as determined by HPLC. Egg SM and POPC were purchased from Avanti Polar Lipids (Alabaster, AL) and Nippon Oil and Fat (Osaka, Japan). All other materials were obtained from commercial sources.

Preparation and characterization of 5A PL complexes

HDL-like 5A-POPC and 5A-SM complexes were prepared by a co-lyophilization procedure (25, 26). Peptide and PLs were dissolved in glacial acetic acid and mixed at 1:1.25 w/w ratio (approximately 1:7 molar ratio) and lyophilized. The powder was hydrated with bicarbonate buffered saline and cycled between 50°C and room temperature to facilitate 5A-lipid binding. The resulting HDL complexes were analyzed by gel permeation chromatography, with UV detection at 220 nm, using a Tosoh TSK gel G3000SWxl column (Tosoh Bioscience, King of Prussia, PA). The HDL hydrodynamic diameters were determined by dynamic light scattering (DLS), using a Zetasizer Nano ZSP (Malvern Instruments, Westborough, MA). The volume intensity average values were reported. The α-helical contents of free and lipid bound 5A peptide were determined by Jasco J715 (Jasco, Easton, MD) circular dichroism spectropolarimeter. Samples at 0.1 mg/ml concentration were loaded into a quartz cuvette (d = 0.2 cm path length), and circular dichroism (CD) spectra from 185 to 240 nm were recorded at 24°C. Data were normalized by calculating the mean residue ellipticity (θ).

Transmission electron microscopy (TEM) images were obtained using a JEM 1200EX electron microscope (JEOL, USA) equipped with an AMT XR-60 digital camera (Advanced Microscopy Techniques Corp.). Images were acquired at magnifications from 60,000- to 150,000-fold. HDL samples, 3 μl aliquots, were deposited on carbon film-coated 400 mesh copper grids (Electron Microscopy Sciences) and dried for 1 min. The samples were negatively stained with 1% uranyl acetate solution; the grids were blotted with tissue and dried before TEM observation.

Cholesterol efflux assay in vitro

Cholesterol efflux studies were performed as described previously (25, 26). Briefly, baby hamster kidney (BHK)-mock and BHK stably transfected cells with human ABCA1 cDNA, ABCG1 cDNA, and SR-BI cDNA were labeled for 24 h with 1 μCi/ml of ^{3}H-cholesterol in minimum essential medium plus 10% fetal calf serum. Transporters were induced with 10 nM mifepristone in DMEM, containing 0.2 mg/ml of fatty acid-free BSA for 18 h. Following induction of the transporters, the cells were washed and rHDLs or 5A were added at 0.1, 2.5, 5, 10, 20, and 40 mM peptide concentrations in DMEM-BSA-mifepristone media. After 18 h of incubation, media were collected and filtered using a 24-well, 25-μm pore size plate filter (Whatman-GE Healthcare, Pittsburg, PA) and cells were lysed in 0.4 ml of 0.1% SDS and 0.1 N NaOH. Radioactive counts in media and cell fractions were measured by liquid scintillation counting, and percent cholesterol effluxed was calculated by dividing the media count by the sum of the media and cell counts.

Plasma HDL remodeling

Remodeling of rHDL in plasma was assessed by addition of 50 μl of 5, 1, or 0.5 mg/ml of 5A-SM or 5A-POPC to 450 μl of pooled human plasma. The final concentrations of peptide in plasma were 0.5, 0.1, and 0.05 mg/ml, respectively. Plasma incubation with the same volume of PBS was used as a control. Samples were incubated at 37°C for 1 h under shaking at 300 rpm prior to electrophoresis. The various subclasses of HDL were separated by

size and charge by 1D or 2D native page gel electrophoresis and visualized by Western blot using anti-ApoA-I antibody.

To visualize native HDL particles separated by size, samples were subjected to electrophoresis using 10-well Tris-borate-EDTA (TBE) gradient (3–25%) acrylamide mini-gels (Jule, Inc., Milford, CT) (28). For each well, 5 μl of rat and human plasma incubated with or without rHDL was mixed with 5 μl of 2× TBE sample buffer and 6 μl of the resulting mixtures were loaded per well. Gels were run at 200 V until the sample dye was 2.5 cm away from the bottom of the gel. Proteins were visualized by Western blot by transfer onto polyvinylidene difluoride membrane and incubation overnight with anti-human and anti-rat ApoA-I-HRP-conjugated antibody (Meridian Life Science, Memphis, TN). Antibody solution was prepared by mixing 3 μl of antibody with 40 ml of antibody dilution buffer. Images were acquired on an Alpha Innotech Chemi Imager 5500 and the Alpha Ease FC program was used for spot densitometry.

To visualize native HDL particles separated by charge and size, samples were subjected to native-native 2D gel electrophoresis (29). For each sample, 2 μl plasma incubated with rHDLs or PBS control, 4 μl sample buffer, and 8 μl Tris tricine buffer were combined. A 10.0 μl aliquot was added per well of the first-dimension gel (0.7% agarose), followed by second-dimension electrophoresis on a 3–25% acrylamide gradient TBE mini-gels (Jule, Inc.). The Western blot analysis and visualization was performed as described above. The classification of various HDL subclasses was performed in accordance with Asztalos, Tani, and Schaefer (30).

Inhibition of cytokine release testing

Inhibition of cytokine release from murine peritoneal macrophages following lipopolysaccharide (LPS) stimulation was determined for 5A-SM, 5A-POPC, free 5A peptide, and PBS controls. Mouse peritoneal lavage was performed with 5 ml of sterile PBS. Peritoneal macrophages were washed, collected by centrifugation, and reconstituted in DMEM containing 10% FBS. Cells were plated, attached, washed twice with PBS, stripped by trypsin, and counted. Macrophages were seeded at 100,000 cells per well and incubated for 2 h, followed by addition of rHDLs at 0.01, 0.1, and 1 mg/ml peptide concentrations for 18 h. The cells were washed again, treated with 1 μg/ml of LPS for 2 h, washed again, and incubated for 6 h. The media were collected and the levels of TNF-α were determined using BioLegend ELISA kits (San Diego, CA) as per the manufacturer's instructions.

Determination of cytokine release inhibition in whole human blood was performed by pretreating heparinized human blood for 1 h with 5A-SM, 5A-POPC, and free 5A peptide controls at 0, 0.01, and 0.1 mg/ml peptide concentrations. Cytokine release was stimulated by addition of 1 μg/ml of phytohemaglutinin-M (PHA) followed by an overnight incubation. The cells were collected by centrifugation and the levels of IL-1β, IL-6, and TNF-α were measured by Human ProInflammatory-4 I tissue culture kit using SECTOR® Imager 2400 from Meso Scale Discovery (Rockville, MD).

Cholesterol mobilization and esterification in vivo

Sprague-Dawley rats (8 weeks old) were purchased form Charles River Breeding Laboratories (Portage, MI) and were fed a regular rodent chow diet. To determine the dose response, 5A-SM and 5A-POPC were administered intravenously via the tail veil at 30 and 100 mg/kg doses based on the peptide amount. The plasma samples were collected predose and at 0.5, 1, 2, 4, 6, 8, 12, and 24 h after the infusion, and the levels of plasma PLs, total cholesterol (TC), and unesterified or free cholesterol (FC) were determined by enzymatic analysis using commercially available kits (Wako Chemicals, Richmond, VA). Cholesterol ester (CE) level was calculated as a difference between TC and FC levels at each time point.

Distribution of mobilized cholesterol in lipoproteins

The rat sera samples were analyzed to assess cholesterol distribution between VLDL, LDL, and HDL lipoprotein fractions. Separation of lipoproteins was performed on a Waters HPLC system equipped with a Superose 6 10/300 GL column (GE Healthcare, Piscataway, NJ) and a fraction collector. Rat sera prior to dosing and 30 min postinjection of 100 mg/ml 5A-SM and 5A-POPC were analyzed. Fifty microliter aliquots were injected and eluted with saline solution at 1 ml/min. Elution fractions (0.5 ml) were collected with a Waters fraction collector and analyzed for TC by an enzymatic kit. The levels of cholesterol were plotted as a function of fraction time.

Anti-atherosclerotic activity in ApoE$^{-/-}$ mice

Eight-week-old male ApoE knockout (ApoE$^{-/-}$) mice were fed a high-fat high-cholesterol diet (21% fat, 34% sucrose, and 0.2% cholesterol; Harlan, T.D. 88137) for 14 weeks to develop atherosclerotic lesions, at which point mice were either euthanized (baseline) or switched to a chow diet for 6 weeks. Coincident with the switch to chow diet, mice were randomized into three groups and received an intraperitoneal injection three times a week (Monday, Wednesday, and Friday) of either 5A-POPC or 5A-SM at 50 mg/kg dose or an equivalent volume (200 μl) of PBS control for 6 weeks. The left ventricle of the heart was perfused with PBS, followed by a fixative solution (4% paraformaldehyde in PBS). The aorta was dissected from its origin in the heart to the ileal bifurcation and stained with oil red O solution, then destained for 30 min in 70% ethanol, and finally washed in water. After removal of any remaining adventitial fat, aortas were cut longitudinally and pinned flat onto a black-wax plate. The percentage of the plaque area stained by oil red O with respect to the total luminal surface area was quantified with ImageJ analysis software. To quantify the extent of the atherosclerotic lesions in the aortic root, the atherosclerotic lesions in the aortic sinus region were examined at three locations, each separated by 80 μm. The largest plaque of the three valve leaflets was adopted for morphological analysis. The lipid-burden plaque areas at the aortic sinus were determined by oil red O staining.

RESULTS

Preparation and characterization of rHDLs

rHDL particles were prepared by combining 5A peptide with either SM or POPC, using a co-lyophilization procedure. Preliminary studies were performed to determine the optimal weight ratio of peptide to PLs for formation of homogeneous rHDL complexes. The ratio of 1:1.25 wt/wt or 1:7 mole:mole of peptide to PL was selected. Higher ratios of lipid to peptide resulted in greater rHDL heterogeneity and the presence of liposome impurities. Lower amounts of lipid resulted in the presence of some lipid-free peptide. The optimum weight ratio of peptide to PL ranged between 1:1.25 and 1:1.5 and resulted in homogenous rHDL particle size distribution. The 1:1.25 ratio was chosen as the preferred formulation.

The analysis of the purity of rHDL complexes was performed by gel permeation chromatography, shown in supplementary Fig. 1. The results indicate formation of rHDL (elutes at 7 min) and a presence of PL-unbound or free 5A peptide (12 min retention time). The POPC-HDL contained

a slightly higher percentage of unbound 5A relative to the SM-HDL preparation. The HDL peak width appeared to be narrower for 5A-SM compared with 5A-POPC, indicating decreased polydispersity of the SM-rHDL particles. Both preparations appeared to be homogeneous in size, as determined by DLS measurement. The volume averaged size distribution and width of distribution were 12.8 and 2.4 nm for POPC-rHDL and 9.6 and 0.7 nm for SM-rHDL. The binding of peptide to PLs was also confirmed by increased helicity of 5A in rHDL particles relative to free peptide by circular dichroism measurement. The α-helix content of lipid-bound 5A was 37.9 ± 0.7% and 37.6 ± 0.4% for POPC and SM rHDL, respectively, versus 18.8 ± 0.3% for the free 5A peptide solution (n = 3, mean ± SD).

The morphology of rHDL particles was observed by TEM with negative staining (**Fig. 1**). Formation of highly homogeneous discoidal shaped rHDL of 8–12 nm diameter was observed for 5A-SM. The 5A-POPC rHDL had slightly larger size, greater heterogeneity, and a less defined shape. Some of these differences could be indicative of lower glass transition temperature of POPC relative to SM.

The effect of rHDL composition on cholesterol efflux in vitro

The effect of the PL composition of rHDL on in vitro cholesterol efflux via ABCA1 (**Fig. 2A**), ABCG1 (Fig. 2B), and SR-BI (Fig. 2C) was examined using BHK cells stably transfected with various human transporters that promote cholesterol efflux. The cells were loaded with radioactive cholesterol and percent cholesterol efflux was determined following incubation with different concentrations of 5A-POPC, 5A-SM, and lipid-free 5A peptide. The ABCA1 transporter is known to primarily promote the cholesterol efflux to lipid-poor or lipid-free ApoA-I and thus was able to also promote cholesterol efflux to lipid-free 5A. Reconstituting 5A with either POPC or SM did not interfere with this process; in fact, both 5A-POPC and 5A-SM showed higher cholesterol efflux than lipid-free 5A and were similar to each other. In contrast, ABCG1 and SR-BI are known to primarily promote cholesterol efflux to HDL and not lipid-free ApoA-I and thus showed relatively low cholesterol efflux to 5A. Reconstituting 5A with either PC or SM showed considerably greater efflux than lipid-free 5A for both the ABCG1- and SR-BI-transfected cell lines. At the highest concentration tested, both rHDL particles made with either SM or POPC were 40–50% more effective cholesterol acceptors from ABCG1- and SR-BI-transfected cells. Similar results, however, were also obtained from the mock-transfected cells, which primarily efflux cholesterol by a passive diffusion process (31), suggesting that the increase in cholesterol efflux to rHDL was largely due to an increase by aqueous diffusion pathway. Although 5A-SM-HDL appeared to have slightly better in vitro efflux capacity than 5A-POPC-HDL for all four cell lines tested; overall, the two rHDL preparations yielded similar results, regardless of the mechanism for cholesterol efflux from cells.

HDL remodeling in plasma

To assess how rHDL interacts with endogenous lipoprotein, 5A-POPC and 5A-SM were incubated with human plasma and HDL remodeling was visualized by 1D and 2D native page electrophoresis. Samples of 5A-SM and 5A-POPC were incubated for 30 min in human plasma at final peptide concentrations of 0.5, 0.1, and 0.05 mg/ml. The HDL subfractions were separated by size by 1D native page electrophoresis (**Fig. 3**). The incubation resulted in a measurable increase in the preβ HDL band at 0.1 mg/ml concentration for 5A-SM and for both rHDL compositions at 0.5 mg/ml concentration. The increase in preβ HDL

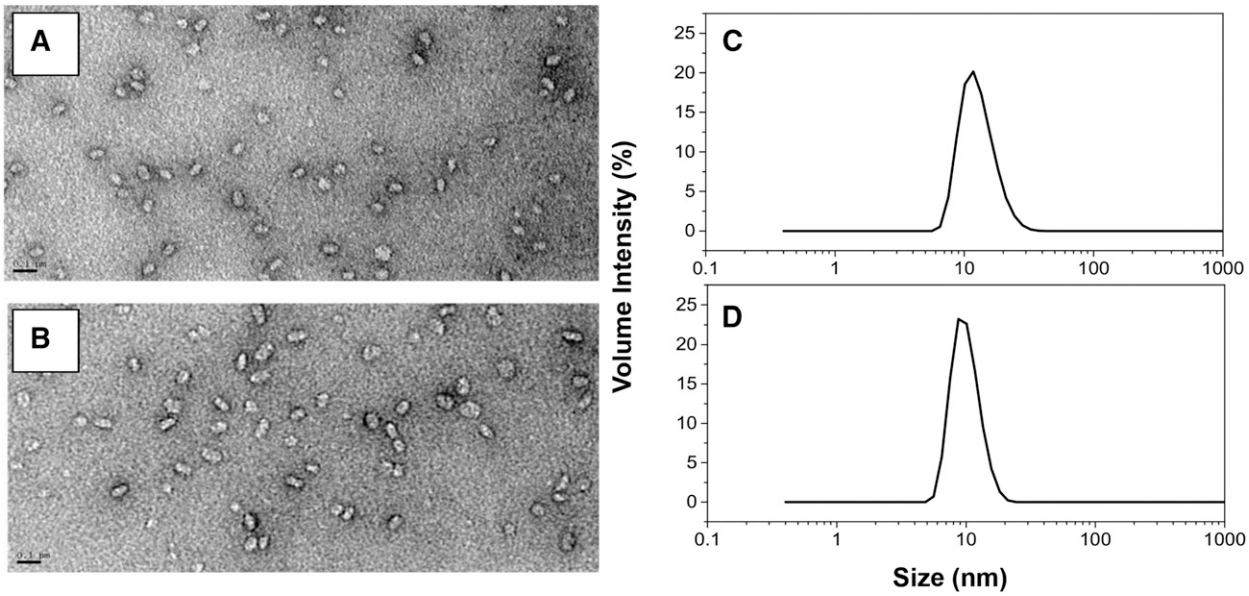

Fig. 1. Electron microscopy images of 5A-SM (A) and 5A-POPC (B), and particle size distribution analyzed by DLS for 5A-SM (C) and 5A-POPC (D). The scale bar corresponds to 0.1 μm.

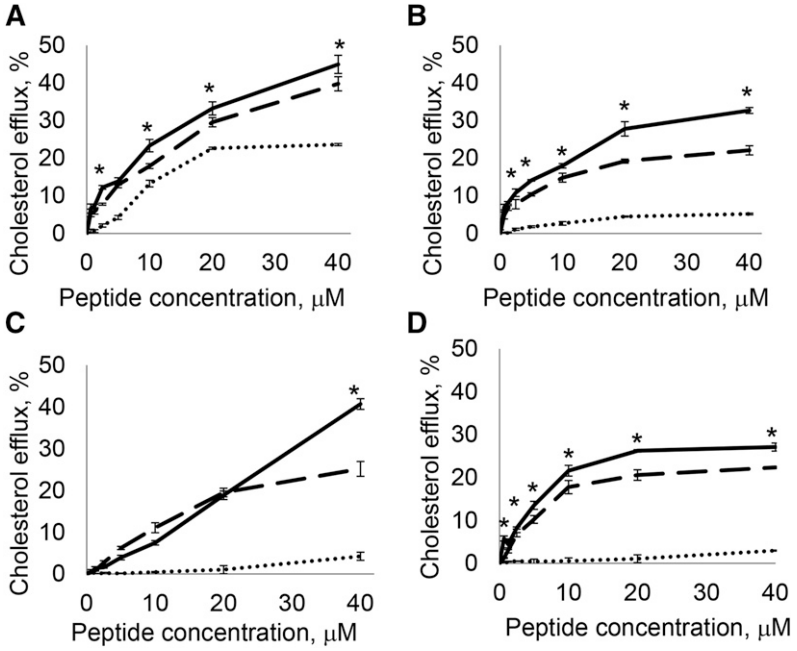

Fig. 2. Concentration dependence of cholesterol efflux by 5A-SM (solid line), 5A-POPC (dashed line), and 5A peptide (dotted line). Percent of cholesterol efflux was determined after 18 h incubation of plasma with BHK cells stably transfected with ABCA1 (A), ABCG1 (B), SR-BI transporters (C), or mock cells (D). Statistically significant differences between 5A-SM and 5A-POPC (*) with *P* values of at least <0.05.

was statistically higher for 5A-SM relative to 5A-POPC at 0.5 mg/ml ($P < 0.05$). The 2D gel analysis of 5A-POPC and 5A-SM incubations at the highest concentration of 0.5 mg/ml confirmed the 1D gel findings (**Fig. 4B**). An increase in preβ HDL (highlighted by dashed circles in Fig. 4)

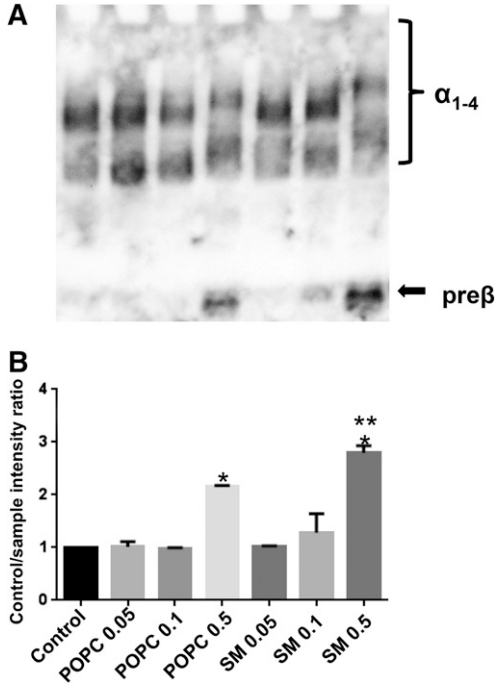

Fig. 3. Human plasma incubation of 5A-POPC and 5A-SM causes HDL remodeling. A: Dose dependent formation of smaller preβ-like HDL (arrow) upon 5A-POPC and 5A-SM incubation with plasma at 0.05, 1, and 0.5 mg/ml relative to PBS control. B: Quantitative analysis of preβ HDL formation in each lane. Statistically significant increase in preβ HDL was observed for incubation with 0.5 mg/ml of both rHDL relative to control (*$P < 0.05$). More preβ is formed following incubation with 5A-SM relative to 5A-POPC (**$P < 0.05$)

was observed for both 5A-POPC and 5A-SM; however, the effect is more prominent for 5A-SM than for 5A-POPC. Similar notable increases in α-1 and α-2 HDL intensities were observed for both rHDL preparations. The incubation of 5A-SM and 5A-POPC with rat plasma also showed complete disappearance of α-HDL spots and appearance of prominent preβ HDL. These findings suggest that both 5A-POPC and 5A-SM can readily interact with native HDL to induce remodeling in plasma. The HDL remodeling was somewhat more prominent upon 5A-SM incubation compared with 5A-POPC, which correlates well with higher anti-atherosclerotic activity in vivo of 5A-SM, shown later in this work.

Anti-inflammatory properties

The effects of PL composition on the anti-inflammatory properties of rHDL were examined in two separate experiments. First, mouse peritoneal macrophages were harvested, plated, and preincubated with 5A-SM or 5A-POPC at 0.01, 0.1, and 1 mg/ml concentrations for 18 h. Following incubation, the medium was replaced with fresh medium without rHDL, and cytokine release was stimulated by addition of LPS. Both lipid formulations of rHDL exhibited dose-dependent inhibition of cytokine release, although 5A-SM appeared to be significantly more potent than 5A-POPC (**Fig. 5A**). Both the high (1 mg/ml) and mid dose (0.1 mg/ml) of 5A-SM almost completely inhibited TNF-α release, while only the 1 mg/ml dose of 5A-POPC showed some protection. It is known that HDL can physically bind and neutralize LPS; however, this protection mechanism is unlikely to be applicable here, because the rHDL-containing medium was removed and a new medium was added prior to LPS stimulation.

The ability of 5A-SM- and 5A-POPC-HDL to inhibit cytokine release in whole human blood stimulated by addition of PHA was also examined. The 5A-POPC and 5A-SM

JOURNAL OF LIPID RESEARCH

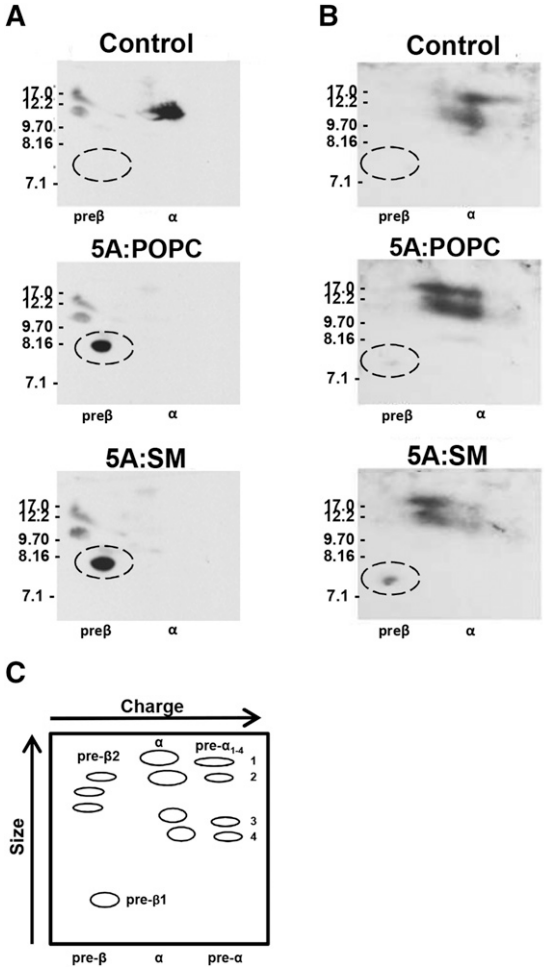

Fig. 4. The 2D gel electrophoresis of rat (A) and human (B) plasma incubated with either PBS control or 0.5 mg/ml of 5A-POPC or 5A-SM. Preβ HDL is highlighted by a dashed line circle. C: Map of various subclasses of HDL according to classification by Asztalos, Tani, and Schaefer (30).

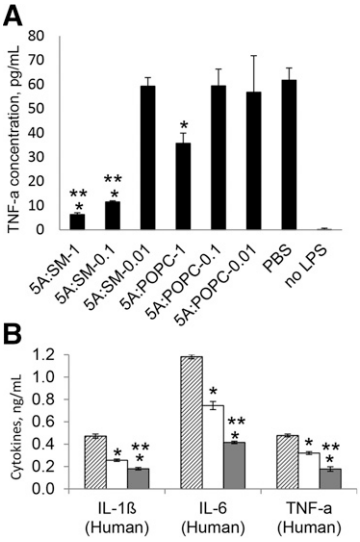

Fig. 5. Inhibition of cytokine release by 5A-POPC and 5A-SM incubation. A: TNF-α release from murine macrophages stimulated by addition of LPS was inhibited by preincubation with 5A-SM at 1 and 0.1 mg/ml and partially inhibited by 5A-POPC at 1 mg/ml. B: Inhibition of cytokine release in whole human blood following PHA stimulation by addition of 0.1 mg/ml of 5A-POPC (white bars) and 5A-SM (solid bars) relative to saline control (lined bars). Statistically significant differences between rHDL and PBS control (*) and between 5A-SM and 5A-POPC (**) with *P* values of at least <0.05.

particles were added at 0, 0.01, and 0.1 mg/ml and preincubated for 1 h. Cytokine release was stimulated with PHA and the levels of IL-1β, IL-6, and TNF-α were determined (Fig. 5B). Similar to the mouse macrophage results, both rHDLs exhibited dose-dependent inhibition of cytokine release relative to buffer control ($P < 0.005$ for 5A-SM and $P < 0.05$ for 5A-POPC), and once again 5A-SM offered better protection relative to 5A-POPC ($P < 0.01$).

Cholesterol mobilization and esterification in vivo

A rat dose-response study was performed in order to evaluate whether apparent differences between 5A-SM- and 5A-POPC-HDL in cholesterol efflux in vitro translate to significant differences in cholesterol mobilization in vivo. Sprague-Dawley rats received 30 and 100 mg/kg doses of 5A-POPC- or 5A-SM-HDL by intravenous infusion. The dose was based on the peptide content of the dosing solutions. The increase in plasma FC, CE, and PL levels is plotted in **Fig. 6A–F**. The amount of mobilized FC was proportional to the injected dose and reached a maximum within 1 to 3 h post infusion, depending on the dose. Most of the mobilized cholesterol appeared to be unesterified. Statistically significant differences in FC increase between 5A-POPC and 5A-SM were observed for 30 and 100 mg/kg doses at almost all time points ($P < 0.05$, noted in Fig. 6). Chromatographic separation of plasma lipoproteins 30 min following rHDL dosing revealed the presence of mobilized cholesterol in its entirety in the HDL fraction, as shown in **Fig. 7**. The analysis confirmed higher levels of mobilized cholesterol in the HDL fraction for the 5A-SM infusion relative to 5A-POPC. Approximately two to three times more cholesterol accumulated in the plasma compartment per dose of injected 5A-SM-HDL relative to 5A-POPC-HDL. The maximum FC mobilization was obtained 3 h postdose for 100 mg/kg, and when FC levels increased from baseline by 105.6 mg/dl for 5A-SM-HDL and by 53.3 mg/dl for 5A-POPC-HDL ($P < 0.01$ for two rHDLs). The baseline level of plasma FC was 30 ± 5 mg/dl, thus the 30 and 100 mg/kg infusions of 5A-SM corresponded to 107 and 387% increases for plasma FC levels, respectively. The same doses of 5A-POPC resulted in 53 and 189% increases for plasma FC, respectively.

The administration of 30 and 100 mg/kg doses of rHDL (based on 5A peptide amount) corresponded to infusion of 37.5 and 125 mg/kg of either POPC or SM, resulting in a significant increase in total circulated plasma PL levels. The level of rat plasma PL prior to infusion was approximately 100–125 mg/ml. The administration of rHDL resulted in initial PL increase by approximately 70–80 mg/ml and 400–440 mg/ml for 30 and 100 mg/kg doses, respectively. The initial PL increase was similar for both 5A-SM and 5A-POPC. While for the 5A-POPC infusion the PL lipid levels decreased according to first-order elimination;

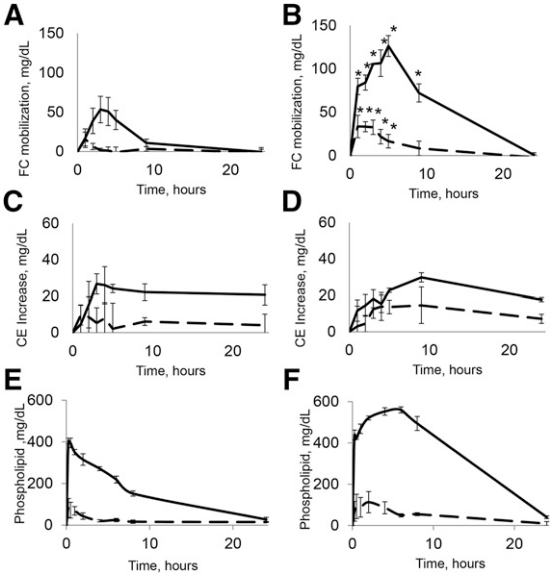

Fig. 6. Dose response of cholesterol mobilization following 5A-POPC and 5A-SM infusions at 30 mg/kg (dashed line) and 100 mg/kg (solid line) in normal rats. Unesterified cholesterol or FC mobilization by 5A-POPC (A) and 5A-SM (B). Increase in CE levels after infusion of 5A-POPC (C) and 5A-SM (D). Increase in PLs after infusion of 5A-POPC (E) or 5A-SM (F). *Denotes statistically significant differences between 5A-POPC and 5A-SM of the same dose with *P* values of at least <0.05.

whereas for 5A-SM, a small additional increase in circulating PL was observed for the first 2–6 h depending on the dose. The differences in PL levels were statistically significant for 5A-SM and 5A-POPC for the 100 mg/kg dose 2–8 h post administration ($P < 0.05$). Overall, the circulating PL levels remained elevated for a longer duration for 5A-SM administration relative to 5A-POPC, most likely due to slower metabolism of SM relative to POPC. This slower PL elimination correlates with longer circulation of mobilized FC (Fig. 6A, B). It is important to note that the plasma PL levels return to predose levels 24 h post administration for both rHDL compositions.

Cholesterol mobilization is the first important step in the reverse cholesterol transport pathway; however, it is important to note that the lipid composition of the rHDL particles also affected cholesterol esterification by LCAT, the second step in reverse cholesterol transport (11, 31).

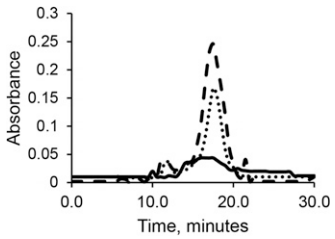

Fig. 7. Infusion of 5A-POPC (dotted line) and 5A-SM (dashed line) leads to rapid cholesterol mobilization in the HDL subfraction 30 min postdose relative to baseline (solid line). Lipoproteins were separated by gel filtration chromatography and cholesterol levels were analyzed post fraction collection. Peaks at 12, 14, and 18 min represent VLDL, LDL, and HDL, respectively.

SM, unlike PCs such as POPC, is not a substrate for LCAT, and some reports indicate that SM inhibits LCAT activity (6). The increase in CE was plotted at each time point following the infusion for each dose of 5A-SM- and 5A-POPC-HDL, as shown in Fig. 6C, D. The dose-dependent increase in CE formation was observed for both 5A-SM and 5A-POPC; however, the absolute amount of CE increase was lower than for FC, indicating that only a small fraction of mobilized FC converts to CE for both HDL compositions. There were no statistically significant differences in CE increase between 5A-POPC and 5A-SM. The CE increase was similar for the 100 mg/kg dose of 5A-POPC and 5A-SM, as well as 30 mg/kg 5A-SM. These results indicate that rapid mobilization of a large amount of FC likely saturates the endogenous LCAT esterification capacity.

Effect of 5A-POPC and 5A-SM rHDL on atherosclerosis regression in mice

The ability of rHDL to reduce the atherosclerotic burden was evaluated for both 5A-POPC and 5A-SM rHDL in ApoE$^{-/-}$ mice. ApoE$^{-/-}$ mice were placed on high-fat diet to develop atherosclerosis (seven to eight animals per group). The baseline control group was euthanized prior to the start of treatment, while the other three groups received intraperitoneal injections of 50 mg/kg 5A-SM, 5A-POPC, or an equivalent volume of PBS administered three times weekly for 6 weeks. Following the conclusion of treatment regimens, animals were euthanized and whole aortas were excised for plaque area analysis by oil red O staining (**Fig. 8**). The baseline en face atheroma area was 22.5% and it increased slightly over the treatment period for the placebo group to 24.1% (Fig. 8A, B). In contrast, the atheroma area was reduced to 20.4% and 16.4% following the treatment with 5A-POPC and 5A-SM, respectively. The relative percent reductions of atheroma area by 5A-SM and 5A-POPC were 28 and 10% compared with baseline. There were no statistically significant differences between 5A-SM and 5A-POPC groups, likely due to the small number of animals and the short duration of treatment. The plaque reduction was statistically significant for 5A-SM-rHDL relative to PBS with $P < 0.01$. Similar results were obtained for aortic root lesions (Fig. 8C, D). The atheroma area following placebo treatment was 30.0% and it was reduced to 24.0 and 20.7% following 5A-POPC and 5A-SM treatment, respectively. The aortic root lesion reduction was statistically significant for 5A-SM treatment relative to PBS ($P < 0.05$). These results suggest that the PL composition of rHDL does indeed affect both cholesterol mobilization in vivo and the anti-atherosclerotic potency of rHDL in the ApoE$^{-/-}$ murine model.

DISCUSSION

The most important finding of this study is the manner and extent to which alteration of rHDL PL composition can alter the biological properties of rHDL, in regard to its cholesterol efflux ability and anti-inflammatory effect. We found that 5A-SM effluxes more cholesterol by SR-BI and ABCG1 mechanisms relatively to 5A-POPC, and this ability

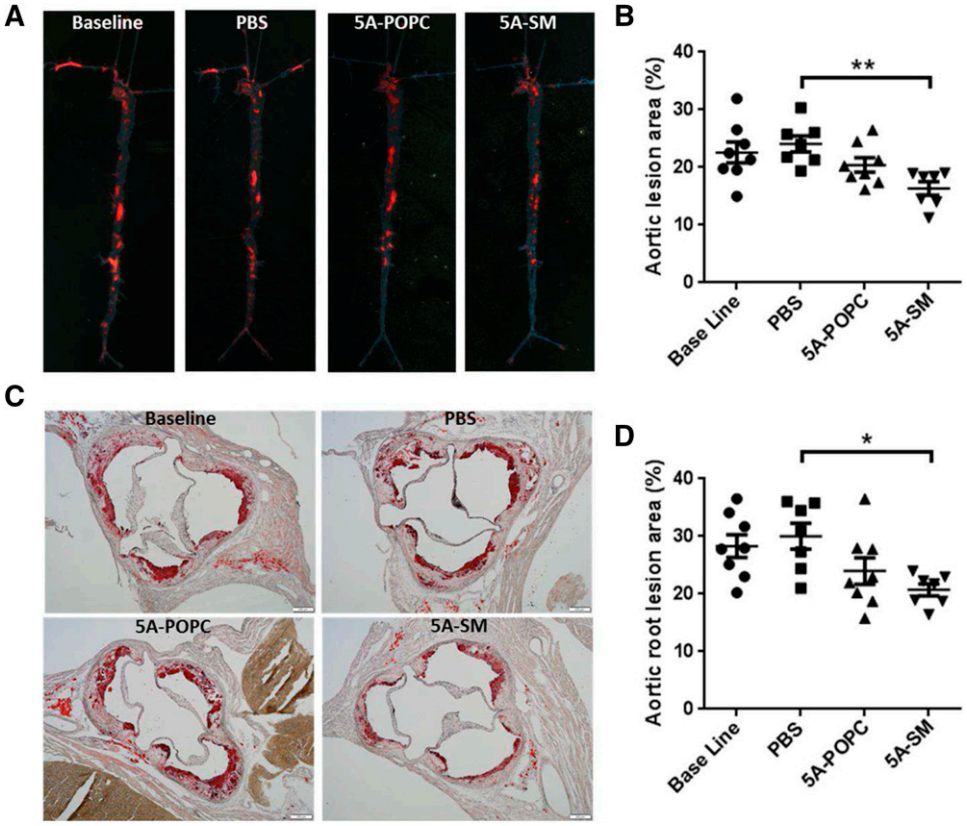

Fig. 8. Effect of 5A-POPC and 5A-SM rHDL on atherosclerosis regression in ApoE$^{-/-}$ mice. Aortas were dissected and plaque areas were visualized by oil red O staining. Representative lesion images and corresponding quantitative analyses of the aortas (A, B) and the aortic root cross-sections (C, D). N = 7–8 animals per group. (*) Denotes statistically significant differences with *P* values of at least <0.05; (**) indicates *P* values of <0.01.

is translated to greater cholesterol efflux capacity by plasma following infusion of rHDLs. ABCA1 efflux was not as much affected by lipid composition, as it is largely driven by lipid-free ApoA-I or the ApoA-I peptide component of HDL. The cholesterol efflux following addition of 5A-POPC and 5A-SM rHDLs to human and rat plasma resulted in lipoprotein remodeling with notable formation of preβ HDL particles. The relative percent of formed preβ HDL was higher for 5A-SM relative to 5A-POPC. The difference between cholesterol efflux ability by ABCG1 and SR-BI for the two rHDL lipid formulations was translated into a notable difference in FC efflux in vivo. The 5A-SM-HDL mobilized roughly twice the amount of cholesterol relative to 5A-POPC-HDL at the same doses (Fig. 6). The mobilized cholesterol was found in the HDL fraction following chromatographic separation of VLDL, LDL, and HDL of a rat plasma sample 30 min post rHDL infusions (Fig. 7). The absolute value of CE increase was similar for both rHDL compositions at high doses, indicating that availability of the endogenous LCAT might be a limiting factor for FC conversion to CE. The conversion of FC to CE following administration of SM-based rHDL was surprising because SM is not a substrate for LCAT, indicating that endogenous PC species are likely to incorporate into SM-based rHDL during remodeling in vivo. Indeed, at the same level of cholesterol mobilization after dosing of either 100 mg/kg of 5A-POPC or 30 mg/kg of 5A-SM, roughly the same percent of FC was converted to CE. All mobilized cholesterol was successfully eliminated by 24 h post rHDL infusion, even after administration of 5A-SM at 100 mg/ml, as lipoprotein parameters returned to a baseline levels. This indicates that rHDL-mobilized cholesterol is most likely eventually eliminated by the liver, either as CE or as unesterified cholesterol. A control experiment to explore cholesterol efflux in vitro and cholesterol mobilization in vivo following administration of POPC or SM vehicles, without addition of ApoA-I mimetic peptide, was not performed in the current study. The administration of lipid vehicles results in cholesterol mobilization and endothelial function modulation, and the relative efficacy depends on the size and lamellar properties of the administered lipid vehicles (32, 33).

The anti-inflammatory properties of rHDL are also affected by lipid composition; 5A-SM was found to inhibit cytokine release in response to LPS more effectively than 5A-POPC. The anti-inflammatory activity differences between 5A-SM and 5A-POPC could be potentially related to the differences in alteration of cellular membrane composition by either passive or SR-BI-mediated efflux. The SR-BI-mediated efflux from the endothelial cells is known to cause activation of eNOS by kinase signaling (34). It is also possible that some of anti- and pro-inflammatory activity of

rHDL is due to small amounts of signaling lipid impurities present in SM and POPC raw materials, such as sphingosine-1-phosphate, sphingosyl-phosphorylcholine, or LPC, or these could be generated after cellular uptake by rHDL. These molecules are known to be potent bioactive signaling molecules and could impact on the inflammatory cascade (34). Another potential mechanism of 5A-POPC- and 5A-SM-related anti-inflammatory activity could be mediated by ABCA1 efflux (35), and related to induction of activating transcription factor 3 (ATF3) transcription modulator (36). The causes for the relative differences between 5A-POPC and 5A-SM anti-inflammatory activities pertaining to these mechanisms have not yet been explored.

Similar differences between SM- and PC-based rHDL were reported in several past studies. ProApoA-I formulated with POPC showed approximately 10-fold lower FC mobilization in the HDL fraction relative to proApoA-I-SM-HDL, following the infusion into New Zealand White rabbits at 15 mg/kg doses (24). The comparison of in vitro cholesterol efflux by ApoA-I and ApoA-I-Milano formulated with either 1,2-dimyristoyl-rac-glycero-3-phosphocholine (DMPC) or SM was conducted in Chinese hamster ovary cells, J774 macrophages, and BHK cells transfected with ABCA1, nonfunctional ABCA1 mutant (W590S), and ABCG1 (9). SM-based rHDL exhibited higher cholesterol efflux than DMPC-based rHDL in all cell systems tested, and the difference was most significant in ABCG1-expressing cells. The PL composition has less effect on ABCA1-mediated efflux, and ApoA-I-Milano-based rHDL was a slightly better cholesterol acceptor relative to ApoA-I-based rHDL. These findings are consistent with ABCA1 and ABCG1 efflux results in our study, using the 5A mimetic peptide.

The effects of PC, fatty acid saturation, and addition of SM to rHDL on cholesterol efflux from J774 macrophages and esterified cholesterol uptake by HepG2 cells were also evaluated by Marmillot, Patel, and Lakshman (8). In general, the highest cholesterol efflux was observed for more saturated lipid-based rHDL, such as fully saturated 1,2-distearoyl-PC (DSPC, 18:0) and 1,2-dioleoyl PC (DOPC, 18:1, mono-unsaturated). The incorporation of egg PC (unsaturated natural mixture), 1,2-dilinoleoyl PC (DLPC, 18:2), and 1,2-dilinolenoyl phosphatidylcholine (DLnPC, 18:3) caused a significant decrease in efflux capacity. The addition of SM increased cholesterol efflux. The CE uptake by HepG2 cells was also higher for rHDL containing more saturated lipids (50–100% of DSPC), while less uptake was observed for egg yolk PC (mostly unsaturated), DOPC, DLPC, and DLnPC. Addition of SM at 40–80% of total lipid decreased the CE uptake by rHDL containing unsaturated lipids, but not for DSPC-based rHDL.

Another study of rHDL lipid composition on cholesterol efflux from mouse L-cell fibroblasts was performed by Davidson et al. (7), but gave slightly different results. The SM-based rHDL exhibited slightly lower efflux capacity than unsaturated POPC- and DOPC-based rHDL. The rHDL based on saturated PCs, such as DSPC (18:0), DPPC (18:0), DMPC (14:0), and 1-palmitoyl-2-stearoyl PC (16:0, 18:0), exhibited lower cholesterol efflux than HDL from POPC and DOPC. This efflux system examines physical uptake of FC from cell membranes similar to the mock efflux measurement in this study. The higher uptake by unsaturated lipids was attributed to the liquid crystalline state of unsaturated lipids at 37°C. However, the duration of rHDL incubation with cells, cell type, and rHDL concentration in the media were different in all the aforementioned studies, thus limiting direct comparison. It is important to note that commercially available SMs are all natural mixtures of lipids purified from different sources. Egg yolk SM, which is composed primarily of palmitic acid (16:0, over 80%), was used in our study, while bovine brain SM (~50% of 18:0 and ~20% of 24:1) was used by Marmillot, Patel, and Lakshman (8) and Davidson et al. (7). Similar to PC, the fatty acid chain length and saturation is expected to affect the cholesterol binding of the SM bilayer and efflux capacity of SM-based rHDL.

An important issue is whether the greater cholesterol mobilization efficiency by SM-based rHDL relative to POPC-based rHDL will result in anti-atherosclerotic efficacy at lower doses. In this study, we did indeed observe a greater anti-atherosclerotic activity of 5A-SM relative to 5A-POPC following administration of eighteen doses of 50 mg/kg of rHDL. Some of our previous data is also supportive of greater activity of SM-containing rHDL relative to POPC-based rHDL (26). In two independent studies, 4-month-old ApoE$^{-/-}$ mice on a normal chow diet were injected with 30 mg/kg of: *i*) 5A:POPC-HDL or POPC liposome control; and *ii*) 5A-SM-DPPC-HDL or saline control for 13 weeks (three times a week) and then analyzed for percentage of surface area covered by aortic plaque. The atheroma area was smaller following 5A-SM-DPPC-HDL treatment (~3.5%) relative to 5A-POPC-HDL treatment (~6%). Injections of both rHDLs showed statistically significant improvement relative to placebo or POPC liposome controls (26). The animal experiment design in the current study involved feeding ApoE$^{-/-}$ mice a high-fat diet for 14 weeks followed by an acute 6 week treatment. The mean atheroma areas were 16.4, 20.4, and 24.1% following 5A-SM-HDL, 5A-POPC-HDL, and placebo treatments, respectively. While the atheroma area was lower following 5A-SM treatment relative to 5A-POPC, the difference was not statistically significant. This lack of a statistically significant difference could be attributed to the low number of animals (seven to eight per group) and the short duration of treatment (6 weeks).

Another critical question is the importance of effective interaction of rHDL with LCAT for successful reduction of atheroma. While SM is not a substrate of LCAT, fully saturated PC, such as DPPC, is capable of serving as a substrate for LCAT and, like SM, is similar in its strong cholesterol binding properties. The unsaturated PCs, such as POPC and DLPC, are reported to be more efficient substrates for LCAT, but unsaturation results in weaker cholesterol efflux. It may be preferable to investigate the effect of lipid composition cholesterol esterification in vivo using either full-length ApoA-I or ApoA-I mimetic peptides optimized specifically for LCAT activation. The results of this study

are significant because they shift the focus of rHDL research from a protein or peptide component to an equally important PL component. While several rHDL products have already been translated to early stage clinical trials, the doses required for clinical efficacy are relatively large (40 mg/kg and 45 mg/kg), requiring as much as 5 g of protein per infusion (4, 5, 15, 16). Administration of such high doses has been associated with toxicity, which may have resulted from various impurities, including cholate used in preparation of sHDL particles, oxidized lipids, potentially immunogenic ApoA-I aggregates, bacterial proteins, DNA, and endotoxins from recombinant processing during manufacturing of ApoA-I. A high dose of 80 mg/kg of CSL-111 also had to be discontinued in a phase 2 study due to toxicity (5). High doses also require the manufacture of large quantities of very pure protein or ApoA-I mimetic peptide and rHDL nanoparticles, which is technically difficult and costly. Hence, the ability to attenuate pharmacological efficacy of rHDL by optimization of its PL composition could potentially lead to the creation of new rHDL therapeutics that are effective at a fraction of the currently used clinical doses.

The end goal of rHDL infusion therapy is to rapidly remove excess cholesterol from arterial plaque and reduce the risk of future heart attack and, therefore, the ability of rHDL to mimic all functions of natural HDL, i.e., endothelial cell layer penetration, cholesterol efflux from foam cells, anti-inflammatory and anti-oxidant functions, interaction with LCAT for conversion of FC to CE, and transport of mobilized and esterified cholesterol to the liver for elimination is highly important. As this study and previously published literature indicate, all of these functions of rHDL are potentially affected by its PL composition. Therefore, understanding the mechanism of how lipid composition alters efficacy and safety of rHDL is critical for successful clinical translation of this novel class of cardiovascular drugs.

The authors wish to acknowledge Biophysics Core Facilities of the National Heart, Lung, and Blood Institute for help with CD spectroscopy and Dr. Georgios Skiniotis and Ms. Annie Dosey from the Life Sciences Institute of the University of Michigan for their help with electron microscopy. The authors would also like to acknowledge KineMed and Nippon Oil and Fat for the gifts of 5A peptide and PLs.

REFERENCES

1. Remaley, A. T., A. Amar, and D. Sviridov. 2008. HDL-replacement therapy: mechanism of action, types of agents and potential clinical indications. *Expert Rev. Cardiovasc. Ther.* **6:** 1203–1215.
2. Newton, R. S., and B. R. Krause. 2002. HDL therapy for the acute treatment of atherosclerosis. *Atheroscler. Suppl.* **3:** 31–38.
3. Badimon, J. J., L. Badimon, and V. Fuster. 1990. Regression of atherosclerotic lesions by high density lipoprotein plasma fraction in the cholesterol-fed rabbit. *J. Clin. Invest.* **85:** 1234–1241.
4. Nissen, S. E., T. Tsunoda, E. M. Tuzcu, P. Schownhagen, M. Yasin, G. M. Eaton, M. A. Laurer, W. S. Sheldon, C. L. Grines, S. Halpern, et al. 2003. Effect of recombinant ApoA-I Milano on coronary atherosclerosis in patients with acute coronary syndromes: a randomized controlled trial. *JAMA.* **290:** 2292–2300.
5. Tardif, J. C., J. Gregoire, P. L. L'Allier, R. Ibrahim, J. Lespérance, T. H. Heinonen, S. Kouz, C. Berry, R. Basser, M-A. Lavoie, et al. 2007. Effects of reconstituted high-density lipoprotein infusions on coronary atherosclerosis: a randomized controlled trial. *JAMA.* **297:** 1675–1682.
6. Rye, K. A., N. J. Hime, and P. J. Barter. 1996. The Influence of sphingomyelin on the structure and function of reconstituted high density lipoproteins. *J. Biol. Chem.* **271:** 4243–4250.
7. Davidson, W. S., K. L. Gillotte, S. Lund-Katz, W. J. Johnson, G. H. Rothblat, and M. C. Phillips. 1995. The effect of high density lipoprotein phospholipid acyl chain composition on the efflux of cellular free cholesterol. *J. Biol. Chem.* **270:** 5882–5890.
8. Marmillot, P., S. Patel, and M. R. Lakshman. 2007. Reverse cholesterol transport is regulated by varying fatty acyl chain saturation and sphingomyelin content in reconstituted high-density lipoproteins. *Metabolism.* **56:** 251–259.
9. Ma, C. I., J. A. Beckstead, A. Thompson, A. Hafiane, R. H. Wang, R. O. Ryan, and R. S. Kiss. 2012. Tweaking the cholesterol efflux capacity of reconstituted HDL. *Biochem. Cell Biol.* **90:** 636–645.
10. Sparks, D. L., W. S. Davidson, S. Lund-Katz, and M. C. Phillips. 1995. Effects of the neutral lipid content of high density lipoprotein on apolipoprotein AI structure and particle stability. *J. Biol. Chem.* **270:** 26910–26917.
11. Parks, J. S., K. W. Huggins, A. K. Gebre, and E. R. Burleson. 2000. Phosphatidylcholine fluidity and structure affect lecithin:cholesterol acyltransferase activity. *J. Lipid Res.* **41:** 546–553.
12. Kontush, A., M. Lhomme, and M. J. Chapman. 2013. Unravelling the complexities of the HDL lipidome. *J. Lipid Res.* **54:** 2950–2963.
13. Camont, L., M. Lhomme, F. Rached, W. Le Goff, A. Nègre-Salvayre, R. Salvayre, C. Calzada, M. Lagarde, M. J. Chapman, and A. Kontush. 2013. Small, dense high-density lipoprotein-3 particles are enriched in negatively charged phospholipids: relevance to cellular cholesterol efflux, antioxidative, antithrombotic, anti-inflammatory, and antiapoptotic functionalities. *Arterioscler. Thromb. Vasc. Biol.* **33:** 2715–2723.
14. Kontush, A., P. Therond, A. Zerrad, M. Couturier, A. Négre-Salvayre, J. A. de Souza, S. Chantepie, and M. J. Chapman. 2007. Preferential sphingosine-1-phosphate enrichment and sphingomyelin depletion are key features of small dense HDL3 particles: relevance to antiapoptotic and antioxidative activities. *Arterioscler. Thromb. Vasc. Biol.* **27:** 1843–1849.
15. Eriksson, M., L. A. Carlson, T. A. Miettinen, and B. Angelin. 1999. Stimulation of fecal steroid excretion after infusion of recombinant proapolipoprotein A-I. Potential reverse cholesterol transport in humans. *Circulation.* **100:** 594–598.
16. Nanjee, M. N., J. E. Doran, P. G. Lerch, and N. E. Miller. 1999. Acute effects of intravenous infusion of ApoA1/phosphatidylcholine discs on plasma lipoproteins in humans. *Arterioscler. Thromb. Vasc. Biol.* **19:** 979–989.
17. Marchesi, M., E. A. Booth, T. Davis, C. L. Bisgaier, and B. R. Lucchesi. 2004. Apolipoprotein A-I-Milano and 1-palmitoyl-2-oleoyl phosphatidylcholine complex (ETC-216) protects the in vivo rabbit heart from regional ischemia-reperfusion injury. *J. Pharmacol. Exp. Ther.* **311:** 1023–1031.
18. Hippalgaonkar, K., S. Majumdar, and V. Kansara. 2010. Injectable lipid emulsions —advancements, opportunities and challenges. *AAPS PharmSciTech.* **11:** 1526–1540.
19. Di Bartolo, B. A., S. J. Nicholls, S. Bao, K. A. Rye, A. K. Heather, P. J. Barter, and C. Bursill. 2011. The apolipoprotein A-I mimetic peptide ETC-642 exhibits anti-inflammatory properties that are comparable to high density lipoproteins. *Atherosclerosis.* **217:** 395–400.
20. Tardy, C., M. Goffinet, N. Boubekeur, R. Ackermann, G. Sy, A. Bluteau, G. Cholez, C. Keyserling, N. Lalwani, J. F. Paolini, et al. 2014. CER-001, a HDL-mimetic, stimulates the reverse lipid transport and atherosclerosis regression in high cholesterol diet-fed LDL-receptor deficient mice. *Atherosclerosis.* **232:** 110–118.
21. Ohvo-Rekilä, H., B. Ramstedt, P. Leppimäki, and J. P. Slotte. 2002. Cholesterol interactions with phospholipids in membranes. *Prog. Lipid Res.* **41:** 66–97.
22. Ramstedt, B., and J. P. Slotte. 1999. Interaction of cholesterol with sphingomyelins and acyl-chain-matched phosphatidylcholines: A comparative study of the effect of the chain length. *Biophys. J.* **76:** 908–915.
23. Silva, L. C., A. H. Futerman, and M. Prieto. 2009. Lipid raft composition modulates sphingomyelinase activity and ceramide-induced membrane physical alterations. *Biophys. J.* **96:** 3210–3222.

24. Dasseux, J-L., T. J. Rea, and A. A. Shenderova, inventors. 2003. Method of treating dyslipidemic disorder. United States patent US 7994120 B2.
25. Sethi, A. A., J. A. Stonik, F. Thomas, S. J. Demosky, M. Amar, E. Neufeld, H. B. Brewer, W. S. Davidson, W. D'Souza, D. Sviridov, et al. 2008. Asymmetry in the lipid affinity of bihelical amphipathic peptides. A structural determinant for the specificity of ABCA1-dependent cholesterol efflux by peptides. *J. Biol. Chem.* **283:** 32273–32282.
26. Amar, M. J. A., W. D'Souza, S. Turner, S. Demosky, D. Sviridov, J. Stonik, J. Luchoomun, J. Voogt, M. Hellerstein, D. Sviridov, et al. 2010. 5A apolipoprotein mimetic peptide promotes cholesterol efflux and reduces atherosclerosis in mice. *J. Pharmacol. Exp. Ther.* **334:** 634–641.
27. Tabet, F., A. T. Remaley, A. I. Segaliny, J. Millet, L. Yan, S. Nakhla, P. J. Barter, K. A. Rye, and G. Lambert. 2010. The 5A apolipoprotein A-I mimetic peptide displays anti-inflammatory and antioxidant properties in vivo and in vitro. *Arterioscler. Thromb. Vasc. Biol.* **30:** 246–252.
28. Freeman, L. A. 2013. Native-native 2D gel electrophoresis for HDL subpopulation analysis. *Methods Mol. Biol.* **1027:** 353–367.
29. Freeman, L. A. 2013. Western blots. *Methods Mol. Biol.* **1027:** 369–385.
30. Asztalos, B. F., M. Tani, and E. J. Schaefer. 2011. Metabolic and functional relevance of HDL subspecies. *Curr. Opin. Lipidol.* **22:** 176–185.
31. Yancey, P. G., A. E. Bortnick, G. Kellner-Weibel, M. de la Llera-Moya, M. Phillips, and G. H. Rothblat. 2003. Importance of different pathways of cellular cholesterol efflux. *Arterioscler. Thromb. Vasc. Biol.* **23:** 712–719.
32. Williams, K. J., R. Scalia, K. D. Mazany, W. V. Rodrigueza, and A. M. Lefer. 2000. Rapid restoration of normal endothelial functions in genetically hyperlipidemic mice by a synthetic mediator of reverse lipid transport. *Arterioscler. Thromb. Vasc. Biol.* **20:** 1033–1039.
33. Rodrigueza, W. V., K. D. Mazany, A. D. Essenburg, M. E. Pape, T. J. Rea, C. L. Bisgaier, and K. J. Williams. 1997. Large versus small unilamellar vesicles mediate reverse cholesterol transport in vivo into two distinct hepatic metabolic pools. Implications for the treatment of atherosclerosis. *Arterioscler. Thromb. Vasc. Biol.* **17:** 2132–2139.
34. Mineo, C., H. Deguchi, J. H. Griffin, and P. W. Shaul. 2006. Endothelial and antithrombotic actions of HDL. *Circ. Res.* **98:** 1352–1364.
35. Zhu, X., J. Y. Lee, J. M. Timmins, J. M. Brown, E. Boudyguina, A. Mulya, A. K. Gebre, M. C. Willingham, E. M. Hiltbold, N. Mishra, et al. 2008. Increased cellular free cholesterol in macrophage-specific Abca1 knock-out mice enhances pro-inflammatory response of macrophages. *J. Biol. Chem.* **283:** 22930–22941.
36. De Nardo, D., L. I. Labzin, H. Kono, R. Seki, S. V. Schmidt, M. Beyer, D. Xu, S. Zimmer, C. Lahrmann, F. A. Schildberg, et al. 2014. High-density lipoprotein mediates anti-inflammatory reprogramming of macrophages via the transcriptional regulator ATF3. *Nat. Immunol.* **15:** 152–160.